

## Cell Lineage-specific Effects Associated with Multiple Deficiencies of Tumor Susceptibility Genes in *Msh2*<sup>-/-</sup>*Rb*<sup>+/-</sup> Mice<sup>1</sup>

Alexander Yu Nikitin, Chia-Yang Liu, Andrea Flesken-Nikitin, Chi-Fen Chen, Phang-Lang Chen, and Wen-Hwa Lee<sup>2</sup>

Department of Molecular Medicine and Institute of Biotechnology, The University of Texas Health Science Center, San Antonio, Texas 78245-3207

### Abstract

Cooperative effects of genetic alterations are frequently observed during carcinogenesis. Mice carrying germ-line mutations in both *Rb* and *p53* or *Msh2* and *p53* die earlier of tumors than mice with only one of these genes inactivated. Mice with a single wild-type *Rb* allele develop a syndrome of multiple neuroendocrine neoplasia, and inactivation of both alleles of *Msh2* gene predisposes mice to gastrointestinal cancer, lymphomas and tumors of the skin that exhibit a mismatch repair defect. Here we showed that *Msh2*<sup>-/-</sup>*Rb*<sup>+/-</sup> mice developed lymphomas later than *Msh2*-deficient littermates, and the lymphomas observed in *Msh2*<sup>-/-</sup>*Rb*<sup>+/-</sup> mice have increased rates of apoptosis and rarely spread to other organs and tissues. In contrast to lymphomagenesis, courses of neuroendocrine, intestinal, and skin carcinogenesis were not significantly influenced by the *Msh2*<sup>-/-</sup>*Rb*<sup>+/-</sup> genetic combination. In these mice, neuroendocrine tumors displayed a loss of the remaining wild-type *Rb* allele but did not show microsatellite instability. On the other hand, the intestinal and skin tumors exhibited microsatellite instability but kept the remaining wild-type allele of *Rb*. Taken together, these data not only revealed a novel biological interaction between *Rb* and *Msh2* but also cell lineage specificity effects associated with multiple deficiencies in these tumor susceptibility genes.

### Introduction

Cancer formation is thought to be a multistage process in which the accumulation of genetic and epigenetic alterations results in selection of the most autonomous and, supposedly, most malignant cell clones (1). It is very cumbersome to sort out the contributions of these multiple genetic alterations during carcinogenesis. Recent progress in developing mouse models of cancer allows better understanding of biological effects resulting from particular combinations of genetic alterations.

Alterations in pathways mediated by *RB*<sup>3</sup> susceptibility gene product are among the most common in human cancer (reviewed in Ref. 2). In humans, the *RB* is inactivated in all familial and sporadic retinoblastomas and in 90% of small cell lung carcinomas (2). Loss of *RB* function also occurs less often in a variety of other human tumors, including osteosarcomas and tumors of the mammary gland and prostate (2).

Mice with a single wild-type *Rb* allele develop a syndrome of multiple neuroendocrine neoplasia (3), which includes *Rb*-deficient melanotroph,  $\alpha$ GSU-containing tumors of the pituitary intermediate and anterior lobes, C-cell thyroid carcinomas, hyperplasia and pheochromocytoma of the adrenal medulla, and parathyroid tumors. The reasons for preferential development of tumors with neuroendocrine

characteristics in *Rb*<sup>+/-</sup> mice remain unclear. However, it is known that there are other factors needed to promote progression of tumors associated with *Rb*-deficiency. For example, the acceleration of carcinogenesis that was observed in *Rb*<sup>+/-</sup> mice with either *p53* (4) or *p27* (5) mutation indicates that additional genetic and/or epigenetic changes must occur. Nevertheless, whether such changes have any specific influences to a given cell type lineage remains to be shown.

*Msh2* (mutS homologue 2) belongs to a group of mammalian DNA mismatch repair genes that are highly conserved homologues of the *Escherichia coli* MutHLS system (6). Mutations of the human *Msh2* have been found in a high proportion of individuals with hereditary nonpolyposis colon cancer, establishing the link between mismatch repair and cancer. Mice with mutations in the *Msh2* gene exhibit a mismatch repair defect and are predisposed to gastrointestinal cancer, lymphomas, and tumors of the skin (reviewed in Ref. 7).

To evaluate genetic interactions between DNA mismatch repair and tumor suppressor genes, *Msh2*-deficient mice were generated and crossed with *Rb*<sup>+/-</sup> mice described earlier (8). Although *Msh2*<sup>-/-</sup>*Rb*<sup>+/-</sup> gene combination did not affect the formation of neuroendocrine, intestinal, and skin neoplasia, development of lymphomas was clearly decelerated. This deceleration was associated with increased apoptosis of lymphoma cells. In agreement with the biologically detrimental effect of the *Msh2*<sup>-/-</sup>*Rb*<sup>+/-</sup> genetic combination, transplantation of embryonic *Msh2*<sup>-/-</sup>*Rb*<sup>-/-</sup> hematopoietic cells to  $\gamma$ -irradiated mice only partially rescued the lethality compared with a near-full rescue when *Msh2*<sup>+/-</sup>*Rb*<sup>+/-</sup> cells were used. These results revealed a novel biological interaction between *Rb* and *Msh2* but also cell lineage specificity effects associated with multiple deficiencies in these tumor susceptibility genes.

### Materials and Methods

**Construction of *Msh2*-targeting Vector.** The mouse *Msh2* gene was isolated from the 129/Sv mouse genomic library (provided by Dr. Tom Doetschman, University of Cincinnati, Cincinnati, OH). Positive clones were subcloned into the pBluescript SK vector (Stratagene). A similar strategy as described previously (8) was used to generate a targeting vector. Briefly, a 9-kb *Bam*HI-*Sal*I fragment of the mouse *Msh2* gene-containing exon 3 was subcloned into the pBluescript SK vector (Stratagene). The *Xho*I fragment containing parts of the exon 3 and downstream intron was deleted and replaced with a *pgkneoA* cassette in the sense orientation. This construct was then subcloned into the p2TK vector to produce the targeting vectors.

**Generation of Mice Carrying the Disrupted *Msh2* Allele.** E14.1 ES cells derived from mouse strain 129/Ola were electroporated, selected, and analyzed by Southern blotting, essentially as described earlier (9). C57BL/6J blastocysts into which 12–14 ES cells were injected were implanted into pseudopregnant F1 (CBA  $\times$  C57BL/6) foster mothers (The Jackson Laboratory, Bar Harbor, ME). Chimeric mice, identified by agouti coat color, were mated with C57BL/6J mice. Offspring with agouti coat color were tested for the presence of the targeted locus by PCR and Southern blotting analysis.

**Mouse Maintenance and Genotyping.** All of the experiments were performed on siblings maintained in the same room and on the same diet. To ensure genetic homogeneity, all of the mice were maintained on C57BL/6J (75%)–129/Ola (25%) backgrounds. The origin and identification of *Rb*<sup>+/-</sup> (8)

Received 6/24/02; accepted 7/31/02.

The costs of publication of this article were defrayed in part by the payment of page charges. This article must therefore be hereby marked *advertisement* in accordance with 18 U.S.C. Section 1734 solely to indicate this fact.

<sup>1</sup> Supported in part by NIH Grants CA58318, CA81020, and EY05785 (to W-H.L.).

<sup>2</sup> To whom requests for reprints should be addressed, at Department of Molecular Medicine and Institute of Biotechnology, The University of Texas Health Science Center, San Antonio, Texas 78245-3207. Phone: (210) 567-7351; Fax: (210) 567-7377; E-mail: leew@uthscsa.edu.

<sup>3</sup> The abbreviations used are: *Rb*, mouse retinoblastoma gene; ES, embryonic stem; MSI, microsatellite(s) instability; BrdUrd, bromodeoxyuridine; AI, apoptotic index.

and *p53*<sup>+/-</sup> (10) mice have been described previously. *Msh2*-deficient mice were identified by multiplex PCR with primers corresponding to sequences of the *Msh2* exon 3, *Msh2*, ex3, 5', 2(5'-TTA AGG CTT CTC CCG GCA ATC TTT C-3') and *Msh2*, ex3, 3' (5'-TAA CCT GCC TCA GTT TCC CCA TGT C-3'), and primers of Neo, 5' and bpA, 3' (11). PCR amplification of DNA from *Msh2*<sup>-/-</sup> or wild-type mice results in 236-bp, or 140-bp DNA fragments, respectively. *Msh2*<sup>+/-</sup> genotype is identified by the simultaneous presence of both fragments. Because both *Rb*- and *Msh2*-deficient mice contain identical *pgkneopA* cassettes, antisense primer corresponding to the PGK promoter region, P<sub>gkpr</sub>,3',3 (5'-TGC ACG AGA CTA GTG AGA CGT GCT A-3') was combined with either *Msh2*,ex3,5',2' or *Rb*,ex20,5',2 (11) primers. The resulting PCR product was 440 bp and 335 bp for *pgkneopA* in *Msh2* and *Rb* gene, respectively. The PCR temperature profile was 94°C for 30 s, 60°C for 1 min, and 72°C for 2 min.

**Collection and Morphological Analyses of Animal Materials.** After anesthesia with avertin, animals were either subjected to cardiac perfusion at 90 mm Hg with phosphate-buffered 4% paraformaldehyde or directly placed in the fixative. All of the major organs were examined during necropsy, and representative specimens were further characterized by microscopic analysis of paraffin sections stained with H&E as described previously (11). Serial sections were performed to identify tumors at early stages of progression (11).

**Evaluation of Cell Proliferation and Apoptosis.** The percentage of proliferating cells was determined by BrdUrd incorporation (BrdUrd index) as described earlier (11). Identification of apoptotic cells (AI) was performed by morphological identification and by the terminal transferase-mediated deoxyuridine nick end labeling (TUNEL) method (11). More than 500 cells were scored to estimate the BrdUrd index and AI.

**PCR Analyses of DNA.** Preparation of cells through microdissection, DNA isolation, and subsequent genotyping were described previously in detail (11). For detection of MSI, primer pairs of D7Mit17-5' and D7Mit17-3', and D14Mit15-5' and D14Mit15-3' were used as described previously (12).

**Generation of  $\gamma$ -irradiated Chimeras.** Transplantation of embryonic hematopoietic cells was performed essentially as described previously (13). Briefly, gestational day 12.5 embryonic livers were mechanically dissociated by pipetting. After wash in PBS, 10<sup>6</sup> of embryonic cells was i.v. injected into adult mice irradiated by  $\gamma$  rays from a <sup>137</sup>Cs source (11 Gy, 2.44 Gy/min) within 4 h after irradiation.

**Statistical Analyses.** All of the statistical analyses were performed with the programs InStat 3.02 and Prism 3.02 (GraphPad Software). Survival fractions were calculated using the Kaplan-Meier method. Survival curves were compared by log-rank Mantel-Haenszel tests. Two-tailed ANOVA was used to compare mean values when appropriate.

## Results

***Msh2*-deficient Mice Succumb to Lymphoma and to Gastrointestinal and Skin Tumors.** To prepare *Msh2*-deficient mice via gene knockout technology, a targeting vector was constructed by deleting a *XhoI* fragment that corresponded to the mouse 3' end of the exon 3 and with subsequent intron sequence (Fig. 1A) and replacing it with a *pgkneopA* cassette in the sense orientation (Fig. 1B). The construct

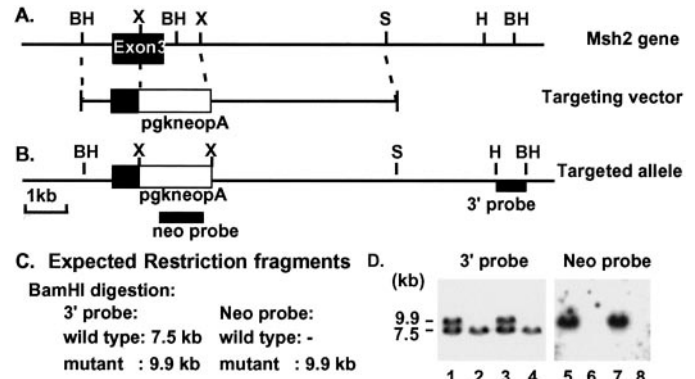


Fig. 1. Generation of a targeted mutation in the mouse *Msh2* gene. A, restriction map of the mouse *Msh2* fragment, encompassing the exon 3 and flanking DNA. A 9-kb *Bam*HI-*Sal*I resistant fragment was used to create the targeting vector. B, structure of a mutant allele after homologous recombination. The probes used for identification of allele-specific recombination are also shown. A 1.2-kb *Xho*I-resistant fragment from the 3' end of exon 3 was deleted and replaced with a *pgkneopA* cassette in the sense orientation with respect to the *Msh2* gene. D, the expected sizes of various restriction fragments detected by 3' flanking and *neo* probes. BH, *Bam*HI; H, *Hind*III; S, *Sal*I; X, *Xho*I.

was cloned into the p2TK vector and transfected into ES cells. Colonies doubly resistant to G418 and FIAU were screened for homologous recombination by Southern blotting (Fig. 1, C and D).

ES cells from clone *Msh2* no. 46 were injected into C57BL/6J blastocysts, which were then implanted into the uteri of pseudopregnant foster mice. From a total of 14 male and 5 female chimeras, 4 male chimeras were used for germ-line transmission. Of the 41 offspring from male chimeras crossed with female C57BL/6J, 46% were heterozygous and 54% were wild type, as shown by PCR analysis of DNA samples. The heterozygous mice were further confirmed by Southern blot analysis of tail DNA samples (data not shown). Heterozygous animals appeared normal, healthy, and were fertile for at least 10 months after birth. After interbreeding of *Msh2*<sup>+/-</sup> mice, 25% (*n* = 15) were *Msh2*<sup>-/-</sup>, 52% (*n* = 32) were *Msh2*<sup>+/-</sup>, and 23% (*n* = 14) were wild type. This closely followed an expected 1:2:1 Mendelian segregation.

Consistent with earlier reports (14, 15), *Msh2*<sup>-/-</sup> mice developed lymphomas and gastrointestinal and skin tumors (Table 1 and Fig. 2). Lymphomas were detected in 75% of the mice and were the predominant cause of death. The majority (90%) of the lymphomas had lymphoblastic B220<sup>+</sup>, CD3e<sup>+</sup> phenotype typical for T-cell origin. Intestinal tumors were detected beginning at P153. Evaluation of the entire gastrointestinal tract revealed that 75% of the animals developed tumors of the small intestine (Table 1). Tumors of the large

Table 1 Incidences of neoplasia in *Msh2*<sup>-/-</sup>, *Msh2*<sup>-/-</sup>*Rb*<sup>+/-</sup>, and *Rb*<sup>+/-</sup> mice<sup>a</sup>

Neoplasia	Genotypes			A <sup>b</sup>	B <sup>c</sup>
	<i>Msh2</i> <sup>-/-</sup> (%)	<i>Msh2</i> <sup>-/-</sup> <i>Rb</i> <sup>+/-</sup> (%)	<i>Rb</i> <sup>+/-</sup> (%)		
Lymphoma	75 (12/16)	68 (15/22)	0 (0/20)	0.7262	
Generalized lymphoma <sup>d</sup>	56 (9/16)	18 (4/22)	0 (0/20)	0.0199	
Tumor of the small intestine	75 (9/12)	79 (11/14)	0 (0/18)	1.0000	
Tumor of the large intestine	33 (4/12)	29 (4/14)	0 (0/18)	1.0000	
Skin tumor	13 (2/16)	9 (2/22)	0 (0/20)	1.0000	
Soft tissue tumor	0 (0/16)	14 (3/22)	0 (0/20)	0.2489	
Melanotroph tumor of the pituitary	0 (0/12)	100 (16/16)	100 (20/20)		ND
Tumor of the pituitary anterior lobe	0 (0/12)	25 (4/16)	26 (5/19)		1.0000
C-cell thyroid carcinoma	0 (0/12)	87 (14/16)	94 (18/19)		0.5820
Adrenal pheochromocytoma	0 (0/12)	69 (11/16)	74 (14/19)		1.0000

<sup>a</sup> Numbers in parentheses indicate number of mice with tumor/total number of mice.

<sup>b</sup> A, Fisher's *P* test *Msh2*<sup>-/-</sup>*Rb*<sup>+/-</sup> versus *Msh2*<sup>-/-</sup>.

<sup>c</sup> B, Fisher's *P* test *Msh2*<sup>-/-</sup>*Rb*<sup>+/-</sup> versus *Rb*<sup>+/-</sup>.

<sup>d</sup> Lymphomas involving more than three tissues were considered as generalized.

<sup>e</sup> ND, not determined.

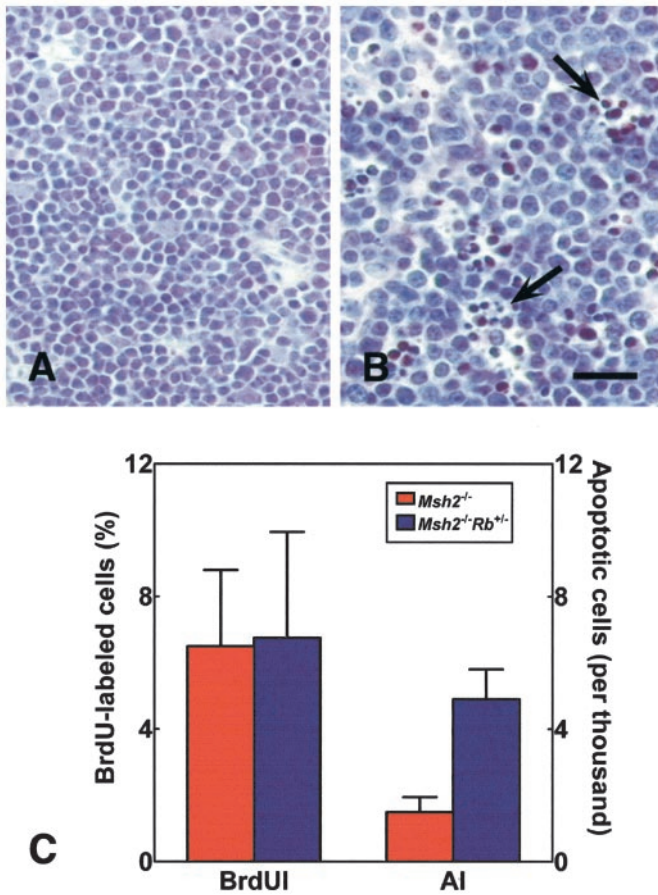


Fig. 2. Characterization of lymphomas in  $Msh2^{-/-}$  and  $Msh2^{-/-}Rb^{+/-}$  mice. *A* and *B*, lymphoblastic lymphomas in  $Msh2^{-/-}$  (*A*) and  $Msh2^{-/-}Rb^{+/-}$  (*B*) mice. Arrows, multiple apoptotic features. H&E staining. Scale bar, 30  $\mu$ m. *C*, quantitation of melanotroph tumor cells synthesizing DNA and undergoing apoptosis. Mice were sacrificed 1 h after injection with BrdUrd. Representative sections of thymic lymphoblastic lymphomas were scored for BrdUrd uptake [BrdUrd index (*BrdUI*), mean  $\pm$  SE] and apoptosis (*AI*, mean  $\pm$  SE) in  $Msh2^{-/-}$  ( $n = 8$ ) and  $Msh2^{-/-}Rb^{+/-}$  mice ( $n = 11$ ). There are different scales for BrdUrd index (%), percent and *AI* (per thousand). Student's *t* test two-tailed  $P = 0.9538$  for BrdUrd index; and  $P = 0.0079$  for *AI* ( $Msh2^{-/-}$  versus  $Msh2^{-/-}Rb^{+/-}$ ).

intestine were identified in 33% of animals. Skin tumors included a basal cell tumor with sebaceous component and a low differentiated squamous cell carcinoma.

**Significantly Longer Life Span of  $Rb^{+/-}Msh2^{-/-}$  Mice Compared with That of  $Msh2^{-/-}$  Littermates.** To evaluate the effects of combined *Msh2* and *Rb* deficiency,  $Rb^{+/-}Msh2^{+/-}$  mice were intercrossed and the life spans of  $Msh2^{-/-}Rb^{+/-}$ ,  $Rb^{+/-}$  and  $Msh2^{-/-}$  littermates were followed. Interestingly,  $Rb^{+/-}Msh2^{-/-}$  mice lived longer when compared with  $Msh2^{-/-}$  littermates ( $P = 0.0003$ ; Fig. 3A). Comparison of the tumors developed in  $Msh2^{-/-}Rb^{+/-}$ ,  $Rb^{+/-}$ , and  $Msh2^{-/-}$  littermates did not reveal any significant differences in either the spectrum of tumors or their incidence (Table 1). However, the spreading of lymphomas was significantly more pronounced in  $Msh2^{-/-}$  mice when compared with  $Msh2^{-/-}Rb^{+/-}$  littermates (Fisher's  $P = 0.0199$ ). At variance with  $Msh2^{-/-}$  mice, 3 soft tissue tumors (myxoid fibrosarcoma, hemangiosarcoma, and hemangioperithelioma) were observed in  $Msh2^{-/-}Rb^{+/-}$  littermates; however, the significance of this observation remains to be clarified because of the small number of soft tissue tumors.

To exclude the possibility that the above phenotype might arise from genetic variations in our mice; similar experiments were performed with  $Rb^{+/-}p53^{-/-}$  mice and their littermates. In agreement with earlier reports (4), mice containing germ-line alterations in both

*p53* and *Rb* had shorter life spans when compared with their littermates with a single gene defect (Fig. 3B).

**High Apoptotic Rate of Lymphoma Cells in  $Msh2^{-/-}Rb^{+/-}$  Mice.** On the basis of earlier studies (15) and our present results, the survival of these animals depended mainly on the progression of lymphomas. To identify reasons for the longer life span of  $Msh2^{-/-}Rb^{+/-}$  mice, proliferation and apoptotic rates of their lymphoma cells were compared with those in  $Msh2^{-/-}$  littermates (Fig. 2). As detected by BrdUrd incorporation, the percentage (mean  $\pm$  SE) of lymphoma cells in S phase of the cell cycle remained similar in mice with either genotype ( $6.75 \pm 3.2\%$ ,  $n = 11$  versus  $6.5 \pm 2.3\%$ ,  $n = 8$ ; Student's *t* test two-tailed  $P = 0.9538$  in  $Msh2^{-/-}Rb^{+/-}$  versus  $Msh2^{-/-}$  mice, respectively). However, the rate of apoptosis was significantly higher in lymphomas of  $Msh2^{-/-}Rb^{+/-}$  mice ( $4.9 \pm 0.9\%$ ,  $n = 11$ , versus  $1.5 \pm 0.45\%$ ,  $n = 8$ ; Student's *t* test two-tailed  $P = 0.0079$  in  $Msh2^{-/-}Rb^{+/-}$  versus  $Msh2^{-/-}$  mice, respectively). Because tumor growth is mainly defined by balance between cell proliferation and apoptosis, the higher apoptotic rate of lymphoma cells is a likely reason for slower growth and progression of lymphomas in  $Msh2^{-/-}Rb^{+/-}$  mice.

**MSI Phenotype Is Not Manifested in Tumors Associated with *Rb* Loss in  $Msh2^{-/-}Rb^{+/-}$  Mice.** MSI is a hallmark of tumors associated with *Msh2* deficiency. It was observed in all lymphomas ( $n = 8$ ) and intestinal tumors ( $n = 10$ ) of  $Msh2^{-/-}$  mice as reported earlier (14, 15). Similarly, MSI was observed in all lymphomas ( $n = 8$ ) and intestinal tumors ( $n = 10$ ) of  $Msh2^{-/-}Rb^{+/-}$  mice. At the same time, neoplasia associated with *Rb* loss of function, such as tumors of the pituitary intermediate lobe ( $n = 6$ ) and anterior lobe

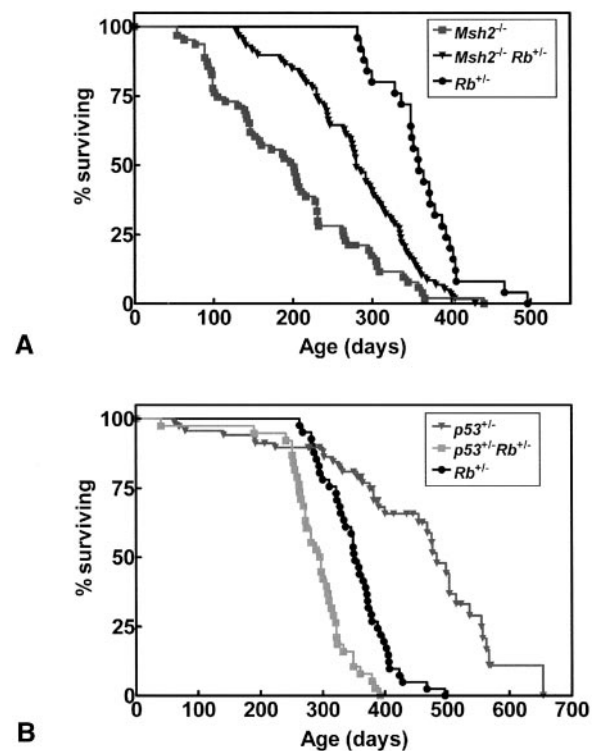


Fig. 3. Life spans of mice with genotypes of  $Msh2^{-/-}$ ,  $Msh2^{-/-}Rb^{+/-}$ ,  $Rb^{+/-}$ ,  $p53^{+/-}$  and  $p53^{+/-}Rb^{+/-}$ . *A*, survival of mice with *Rb* and *Msh2* alterations. Median survivals were 201, 280, and 359 days for  $Msh2^{+/-}$  ( $n = 63$ ),  $Msh2^{-/-}Rb^{+/-}$  ( $n = 59$ ), and  $Rb^{+/-}$  ( $n = 25$ ) mice. ( $P = 0.8982$ ).  $P = 0.0003$  and  $<0.0001$  for log-rank comparisons of survival curves  $Msh2^{-/-}$  versus  $Msh2^{-/-}Rb^{+/-}$  and  $Msh2^{-/-}Rb^{+/-}$  versus  $Rb^{+/-}$ , respectively. *B*, survival of mice with *Rb* and *p53* alterations. Median survivals were 352, 297, and 483 days for  $Rb^{+/-}$  ( $n = 41$ ),  $p53^{+/-}Rb^{+/-}$  ( $n = 38$ ), and  $p53^{+/-}$  ( $n = 68$ ).  $P < 0.0001$  for log-rank comparisons of survival curves of both  $Rb^{+/-}$  versus  $p53^{+/-}Rb^{+/-}$  and  $p53^{+/-}Rb^{+/-}$  versus  $p53^{+/-}$ .

(*n* = 4), the thyroid gland (*n* = 6), and the adrenal gland (*n* = 5) had no detectable change in the length of microsatellites (Fig. 4A, and not shown).

The loss of the *Rb* gene is a rate-limiting event for a number of human and mouse cancers. All neuroendocrine tumors in *Rb*<sup>+/-</sup> mice do not contain wild-type allele at the earliest stages of carcinogenesis (11). In agreement with those observations, genotyping of cells microdissected from tumors of the pituitary intermediate lobe (*n* = 6) and anterior lobe (*n* = 4), the thyroid gland (*n* = 6), and the adrenal gland (*n* = 5) of *Msh2*<sup>-/-</sup>*Rb*<sup>+/-</sup> mice (Fig. 4B and not shown) revealed the presence of only *Rb* mutant alleles. At the same time, no loss of the wild-type allele was observed in any lymphoma (*n* = 9), small intestine adenocarcinoma (*n* = 5), colon adenocarcinoma (*n* = 4), skin squamous adenocarcinoma (*n* = 2), or soft tissue tumors (*n* = 3) of *Msh2*<sup>-/-</sup>*Rb*<sup>+/-</sup> mice (Fig. 4B and not shown).

**Ability of Hematopoietic Cells Deficient for Both *Msh2* and *Rb* is Compromised in Rescuing Lethally Irradiated Mice.** In earlier experiments with *Rb*<sup>+/+</sup>/*Rb*<sup>-/-</sup> chimeras (16), *Rb*<sup>-/-</sup> ES cells contributed extensively to most of the tissues in adult animals. Similarly, *Rb*-deficient hematopoietic cells were able to rescue lethally irradiated mice with an efficiency comparable with that of wild-type cells (13). Hematopoietic development in *Msh2*<sup>-/-</sup> mice appears to be normal (14). However, because of the potential interaction between *Rb* and *Msh2*, the functional status of *Msh2*<sup>-/-</sup>*Rb*<sup>-/-</sup> hematopoietic cells was evaluated. Liver cells of gestational day 12.5 *Msh2*<sup>-/-</sup>*Rb*<sup>-/-</sup> embryos were transplanted into lethally irradiated mice. All of the control mice without transplantation died no later than 15 days after  $\gamma$  irradiation (Fig. 5). However, 90% (9 of 10) mice rescued with *Msh2*<sup>+/-</sup>*Rb*<sup>+/-</sup> cells survived over 221 days after irradiation. In three of four cases, *Msh2*<sup>-/-</sup>*Rb*<sup>-/-</sup> cells protected irradiated mice from lethality at the beginning, but all of the animals died before 170 days after irradiation. The ability of *Msh2*<sup>-/-</sup>*Rb*<sup>+/-</sup> hematopoietic cells in rescuing these irradiated mice appeared to be intermediate (Fig. 5). Taken together, these experiments indicated the biological incompetence of hematopoietic cells deficient for both *Msh2* and *Rb*, suggesting a synthetic function of these two genes.

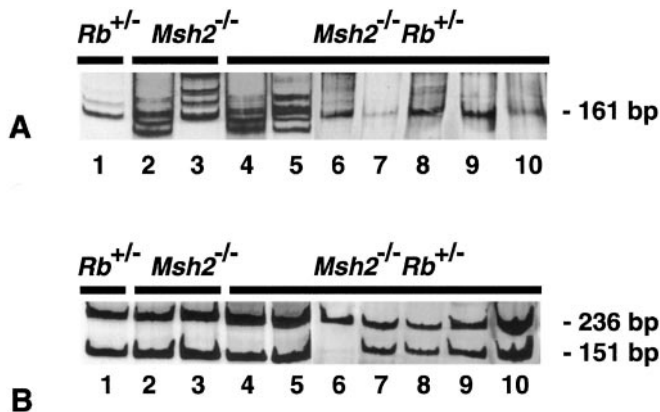


Fig. 4. MSI and loss of heterozygosity of *Rb* in tumors of *Msh2*<sup>-/-</sup> and *Msh2*<sup>-/-</sup>*Rb*<sup>+/-</sup> mice. A, MSI at *D7Mit17* locus in lymphomas and jejunal adenocarcinomas of *Msh2*<sup>-/-</sup> (Lanes 2 and 3, respectively) and *Msh2*<sup>-/-</sup>*Rb*<sup>+/-</sup> mice (Lanes 4 and 5, respectively), but not in the normal thymus of *Rb*<sup>+/-</sup> mouse (Lane 1), in tumors of the anterior (Lane 6) and melanotroph tumors (Lanes 7 and 8) of the pituitary, thyroid C-cell carcinoma (Lane 9) and normal colon epithelium of *Msh2*<sup>-/-</sup>*Rb*<sup>+/-</sup> mice (Lane 10). B, absence of the wild-type *Rb* allele (151-bp PCR product) in thyroid C-cell carcinoma of *Msh2*<sup>-/-</sup>*Rb*<sup>+/-</sup> mouse (Lane 6) but not in the normal thymus of *Rb*<sup>+/-</sup> mice (Lane 1), lymphomas of *Msh2*<sup>-/-</sup>, and *Msh2*<sup>-/-</sup>*Rb*<sup>+/-</sup> mice (Lanes 2, 3, and 4, 5, respectively), jejunal and colon adenocarcinomas (Lanes 7 and 8, respectively), squamous carcinoma of the skin (Lane 9), and hemangiosarcoma (Lane 10) of *Msh2*<sup>-/-</sup>*Rb*<sup>+/-</sup> mice. PCR DNA fragments were analyzed by nondenaturing 12% polyacrylamide gel stained with silver. The 236-bp band corresponds to the mutant *Rb* allele (11).

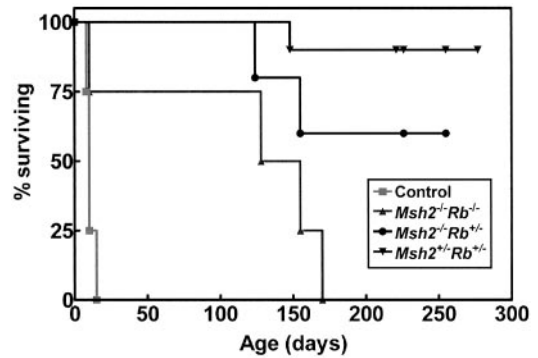


Fig. 5. Survival of mice rescued with *Msh2*<sup>-/-</sup> and *Msh2*<sup>-/-</sup>*Rb*<sup>+/-</sup> hematopoietic cells. Median survivals were 141, undefined, undefined, and 10 days for mice rescued by *Msh2*<sup>-/-</sup>*Rb*<sup>+/-</sup> (*n* = 4), *Msh2*<sup>+/-</sup>*Rb*<sup>+/-</sup> (*n* = 10), *Msh2*<sup>-/-</sup>*Rb*<sup>+/-</sup> (*n* = 5), and control (nonrescued; *n* = 4) mice, respectively. *P* = 0.0005 for log-rank comparison of survival curves *Msh2*<sup>-/-</sup>*Rb*<sup>-/-</sup> versus *Msh2*<sup>+/-</sup>*Rb*<sup>+/-</sup>.

## Discussion

Synergistic effects of genetic alterations are frequently observed during cancer progression. Examples are seen in mice with germ-line mutations in both *Rb* and *p53* or *Msh2* and *p53*, and they die much earlier of tumors than when only a single gene is inactivated. Here we observed that *Msh2*<sup>-/-</sup>*Rb*<sup>+/-</sup> mice developed lymphomas later than *Msh2*-deficient littermates and died much later. This phenotype is explained by the finding that lymphoblasts of these mice have an increased rate of apoptosis and rarely spread to other organs and tissues, as compared with those in *Msh2*<sup>-/-</sup> littermates. Interestingly, loss of the remaining wild-type *Rb* allele did not occur in lymphomas derived from *Msh2*<sup>-/-</sup>*Rb*<sup>+/-</sup> mice but occurred in neuroendocrine tumors. However, MSI was manifested in lymphoma and in intestinal and skin tumors but not in neuroendocrine tumors. These results revealed the cell lineage specificity of biological effects associated with multiple deficiencies in tumor susceptibility genes.

Simultaneous deficiency of *Msh2* and *Rb* may be detrimental for malignant transformation depending on the context of a particular cell lineage. In the lymphoid cell lineage, deceleration of lymphomagenesis is likely attributable to the higher apoptotic rate of lymphoblasts in *Msh2*<sup>-/-</sup>*Rb*<sup>+/-</sup> mice. Whether loss of the remaining wild-type copy of *Rb* is required for decreased survival of *Msh2*<sup>-/-</sup> lymphoblasts remains to be clarified. To substantiate this point is quite difficult because the dead lymphoblasts would not be available for analysis. Nevertheless, because both genes have been implicated in cell-type-specific control of apoptosis (17), and because the *Msh2*<sup>-/-</sup>*Rb*<sup>-/-</sup> hematopoietic cells could not rescue the  $\gamma$ -irradiated mice as described above, it suggested that lymphoblasts with inactivated *msh2* and *Rb* have an apparent deficiency in development. Alternatively, the death of lymphoblasts could simply be attributed to the haploinsufficiency of *Rb*, which may be an adequate requirement that leads to another as-yet-undefined aberrance. In contrast to the deceleration of lymphomagenesis in our *Msh2*<sup>-/-</sup>*Rb*<sup>+/-</sup> mice, surviving *Msh2*<sup>-/-</sup>*p53*<sup>-/-</sup> mice succumbed to thymic tumors significantly earlier than either *Msh2*<sup>-/-</sup> or *p53*<sup>-/-</sup> littermates (18).

The absence of MSI in the neuroendocrine tumors of *Msh2*<sup>-/-</sup>*Rb*<sup>+/-</sup> mice is particularly intriguing. Because the remaining wild-type allele of *Rb* was lost in these tumors but not in the colon tumors and lymphoma that showed MSI, it seems that the presence of *Rb* is inversely correlated with MSI. The molecular basis of this phenotype remains elusive because it is not known whether *Rb* has any regulatory role in the *Msh2* mismatch repair pathway.

Despite the fact that the MSI phenotype is suppressed in these neuroendocrine tumors, it does not necessarily mean that *Msh2* defi-

ciency has no role in these neoplasms. For example, the frequency of MSI in tumors from *Msh2*<sup>-/-</sup>*p53*<sup>-/-</sup> mice is not significantly different from that in *Msh2*<sup>-/-</sup> mice. Nevertheless, tumors did develop faster (18). These results indicated that there is a synergetic biological effect of *Msh2* and *p53* in lymphoblasts. However, whether this synergetic effect occurs in other cell lineages remains to be shown. On the basis of our studies of *Msh2*<sup>-/-</sup>*Rb*<sup>+/-</sup> mice, tumors other than lymphomas did not show any evidence for changes either in proliferation or in apoptosis or differentiation (not shown).

Recent evidence suggested that Rb participates in mitosis and maintains chromosomal stability (19, 20), whereas Msh2 is important for protecting against MSI. Interestingly, at least in colorectal and endometrial cancers, there is an inverse relationship between microsatellite and chromosomal instabilities (reviewed in Ref. 21). Thus, deceleration of lymphomas in *Msh2*<sup>-/-</sup>*Rb*<sup>+/-</sup> mice may represent a model for additional studies of genetic interactions between these two types of instabilities.

The discovery of tumor susceptibility genes has provided a rational approach to cancer prevention and treatment (2). Recent studies demonstrated that prevention of carcinogenesis is achieved by correction of gene copy number in *Rb*<sup>+/-</sup> mice, and the reconstitution of Rb gene functions is sufficient for suppression of neoplasia in immunocompetent mice (22). *Msh2* likely participates in the indirect prevention of neoplasms by maintaining genomic stability mainly on the level of mismatch repair (21). Because carcinogenesis is usually thought of as a multistage process based on an accumulation of multiple genetic and epigenetic alterations (1), gene therapy of tumors at advanced stages may require the targeting of multiple genes. Our earlier studies indicated that in neuroendocrine neoplasia, reconstitution of Rb function is sufficient for suppression of even advanced stages of carcinogenesis, despite the substantial period of time that elapses between tumor initiation and the development of metastatic potential, during which numerous genetic alterations can accumulate (3). Similarly, continuous expression of *H-Ras* and *c-Myc* are required to maintain, respectively, melanoma (23) and papillomatosis (24) formations in mice. At the same time, carcinogenesis in the salivary gland may be abrogated by termination of SV40 large T antigen expression only until a certain stage has been achieved (25). Thus, suppression of the tumor phenotype may depend on gene function in the context of a particular cell lineage.

As demonstrated in the present study, continuous requirement for Rb deficiency during carcinogenesis may prevent genetic selection of some other mutations, such as *Msh2*, which in that particular context may be disadvantageous for neoplastic growth. Further evaluation of genetic interactions between *Msh2* and Rb may result in the identification of the molecular mechanisms suitable for the development of the next generation of therapeutic and prognostic approaches aimed directly toward the attenuation of gene function in tumors of specific cell types.

## Acknowledgments

We thank Nicholas Ting for his critical comments.

## References

1. Fearon, E. R., and Vogelstein, B. A genetic model for colorectal tumorigenesis. *Cell*, 61: 759–767, 1990.
2. Riley, D. J., Lee, E. Y., and Lee, W-H. The retinoblastoma protein: more than a tumor suppressor. *Annu. Rev. Cell Biol.*, 10: 1–29, 1994.
3. Nikitin, A. Y., Juarez-Perez, M. I., Li, S., Huang, L., and Lee, W-H. RB-mediated suppression of spontaneous multiple neuroendocrine neoplasia and lung metastases in *Rb*<sup>+/-</sup> mice. *Proc. Natl. Acad. Sci. USA*, 96: 3916–3921, 1999.
4. Williams, B. O., Remington, L., Albert, D. M., Mukai, S., Bronson, R. T., and Jacks, T. Cooperative tumorigenic effects of germline mutations in Rb and p53. *Nat. Genet.*, 7: 480–484, 1994.
5. Park, M. S., Rosai, J., Nguyen, H. T., Capodieci, P., Cordon-Cardo, C., and Koff, A. p27 and Rb are on overlapping pathways suppressing tumorigenesis in mice. *Proc. Natl. Acad. Sci. USA*, 96: 6382–6387, 1999.
6. Fishel, R., and Wilson, T. MutS homologs in mammalian cells. *Curr. Opin. Genet. Dev.*, 7: 105–113, 1997.
7. Heyer, J., Yang, K., Lipkin, M., Edelman, W., and Kucherlapati, R. Mouse models for colorectal cancer. *Oncogene*, 18: 5325–5333, 1999.
8. Lee, E. Y-H. P., Chang, C-Y., Hu, N., Wang, Y-C. J., Lai, C-C., Herrup, K., Lee, W-H., and Bradley, A. Mice deficient for Rb are nonviable and show defects in neurogenesis and haematopoiesis. *Nature (Lond.)*, 359: 288–294, 1992.
9. Liu, C. Y., Flesken-Nikitin, A., Li, S., Zeng, Y. Y., and Lee, W. H. Inactivation of the mouse *Brcal* gene leads to failure in the morphogenesis of the egg cylinder in early postimplantation development. *Genes Dev.*, 10: 1835–1843, 1996.
10. Donehower, L. A., Harvey, M., Slagle, B. L., McArthur, M. J., Montgomery, C. A. J., Butel, J. S., and Bradley, A. Mice deficient for p53 are developmentally normal but susceptible to spontaneous tumours. *Nature (Lond.)*, 356: 215–221, 1992.
11. Nikitin, A. Y., and Lee, W-H. Early loss of the retinoblastoma gene is associated with impaired growth inhibitory innervation during melanotroph carcinogenesis in *Rb*<sup>+/-</sup> mice. *Genes Dev.*, 10: 1870–1879, 1996.
12. Dietrich, W. F., Miller, J. C., Steen, R. G., Merchant, M., Damron, D., Nahf, R., Gross, A., Joyce, D. C., Wessel, M., and Dredge, R. D. *et al.* A genetic map of the mouse with 4,006 simple sequence length polymorphisms. *Nat. Genet.*, 7: 220–245, 1994.
13. Hu, N. P., Gulley, M. L., Kung, J. T., and Lee, E. Y-H. P. Retinoblastoma gene deficiency has mitogenic but not tumorigenic effects on erythropoiesis. *Cancer Res.*, 57: 4123–4129, 1997.
14. de Wind, N., Dekker, M., Berns, A., Radman, M., and te Riele, H. Inactivation of the mouse *Msh2* gene results in mismatch repair deficiency, methylation tolerance, hyperrecombination, and predisposition to cancer. *Cell*, 82: 321–330, 1995.
15. Reitmair, A. H., Schmits, R., Ewel, A., Bapat, B., Redston, M., Mitri, A., Waterhouse, P., Mittrucker, H. W., Wakeham, A., Liu, B., *et al.* *MSH2* deficient mice are viable and susceptible to lymphoid tumours. *Nat. Genet.*, 11: 64–70, 1995.
16. Williams, B. O., Schmitt, E. M., Remington, L., Bronson, R. T., Albert, D. M., Weinberg, R. A., and Jacks, T. Extensive contribution of Rb-deficient cells to adult chimeric mice with limited histopathological consequences. *EMBO J.*, 13: 4251–4259, 1994.
17. Lee, E. Y., Hu, N., Yuan, S. S., Cox, L. A., Bradley, A., Lee, W. H., and Herrup, K. Dual roles of the retinoblastoma protein in cell cycle regulation and neuron differentiation. *Genes Dev.*, 8: 2008–2021, 1994.
18. Cranston, A., Bocker, T., Reitmair, A., Palazzo, J., Wilson, T., Mak, T., and Fishel, R. Female embryonic lethality in mice nullizygous for both *Msh2* and *p53*. *Nat. Genet.*, 17: 114–118, 1997.
19. Zheng, L., Chen, Y., Riley, D. J., Chen, P-L., and Lee, W-H. Retinoblastoma protein enhances the fidelity of chromosome segregation mediated by hHec1p. *Mol. Cell. Biol.*, 20: 3529–3537, 2000.
20. Zheng, L., Flesken-Nikitin, A., Chen, P-L., and Lee, W-H. Deficiency of *Retinoblastoma* gene in mouse embryonic stem cells leads to genetic instability. *Cancer Res.*, 62: 2498–2502, 2002.
21. Lengauer, C., Kinzler, K. W., and Vogelstein, B. Genetic instability in colorectal cancers. *Nature (Lond.)*, 386: 623–627, 1997.
22. Riley, D. J., Nikitin, A. Y., and Lee, W-H. Adenovirus-mediated *Retinoblastoma* gene therapy suppresses spontaneous pituitary melanotroph tumors in *Rb*<sup>+/-</sup> mice. *Nat. Med.*, 2: 1316–1321, 1996.
23. Chin, L., Tam, A., Pomerantz, J., Wong, M., Holash, J., Bardeesy, N., Shen, Q., O'Hagan, R., Pantginis, J., Zhou, H., Horner, J. W. 2nd, Cordon-Cardo, C., Yancopoulos, G. D., and DePinho, R. A. Essential role for oncogenic *Ras* in tumour maintenance. *Nature (Lond.)*, 400: 468–472, 1999.
24. Pelengaris, S., Littlewood, T., Khan, M., Elia, G., and Evan, G. Reversible activation of *c-Myc* in skin: induction of a complex neoplastic phenotype by a single oncogenic lesion. *Mol. Cell*, 3: 565–577, 1999.
25. Ewald, D., Li, M., Efrat, S., Auer, G., Wall, R. J., Furth, P. A., and Hennighausen, L. Time-sensitive reversal of hyperplasia in transgenic mice expressing SV40 T antigen. *Science (Wash. DC)*, 273: 1384–1386, 1996.